PRIFYSGOL BANGOR / BANGOR UNIVERSITY

PRIFYSGOL
BANGOR
UNIVERSITY

Neighbours matter and the weak succumb: Ash dieback infection is more severe in ash trees with fewer conspecific neighbours and lower prior growth rate

Cracknell, David; Peterken, George; Pommerening, Arne; Lawrence, Peter; Healey, John

Journal of Ecology

DOI:
10.1111/1365-2745.14191

Published: 15/09/2023

Cyswllt i'r cyhoeddiad / Link to publication

Dyfyniad o'r fersiwn a gyhoeddwyd / Citation for published version (APA):
Cracknell, D., Peterken, G., Pommerening, A., Lawrence, P., & Healey, J. (2023). Neighbours matter and the weak succumb: Ash dieback infection is more severe in ash trees with fewer conspecific neighbours and lower prior growth rate. *Journal of Ecology*, *111*(10), 2118-2133. https://doi.org/10.1111/1365-2745.14191

Hawliau Cyffredinol / General rights
Copyright and moral rights for the publications made accessible in the public portal are retained by the authors and/or other copyright owners and it is a condition of accessing publications that users recognise and abide by the legal requirements associated with these rights.

• Users may download and print one copy of any publication from the public portal for the purpose of private study or research.
• You may not further distribute the material or use it for any profit-making activity or commercial gain
• You may freely distribute the URL identifying the publication in the public portal ?

Take down policy
If you believe that this document breaches copyright please contact us providing details, and we will remove access to the work immediately and investigate your claim.

18. Nov. 2024

Neighbours matter and the weak succumb: ash dieback infection is more severe in ash trees with fewer conspecific neighbours and lower prior growth rate

ABSTRACT

1. The epidemiology and severity of ash dieback (ADB), the disease caused by the ascomycete fungus *Hymenoscyphus fraxineus*, has been linked to a variety of site conditions, however, there has been a lack of analysis at an individual-tree scale.
2. Symptoms of ADB were scored on ca. 400 trees of *Fraxinus excelsior* (ash) in permanent sample plots during two successive years in a UK natural woodland reserve. Using comprehensive plot records maintained since 1945, and detailed spatial records updated since 1977, we assembled an array of potential explanatory variables, including site environment factors, ash tree density, previous and present tree condition and near neighbourhood summary statistics (NNSS), such as species mingling and size dominance. Their impact on the severity of ADB of focal ash trees was tested with generalised linear mixed effects models (GLMM).
3. The severity of ADB was much greater in the lower slope parts of the site with moister soils and least in a managed area subject to tree thinning in the previous 35 years. Severity of ADB had a negative association with focal ash tree prior relative growth rate over a period of a decade immediately before the disease was detected at the site. Greater ADB severity was also significantly associated with smaller diameter at breast height of ash trees. Additionally, ADB was significantly positively associated with a greater proportion of heterospecific trees amongst the six nearest neighbours of the focal tree.
4. *Synthesis.* The relationship of the severity of ADB disease with site environment, tree condition and neighbourhood is complex but nevertheless important in the progression of the

disease. The findings suggest some silvicultural interventions, such as thinning to increase the vigour of retained ash trees, might reduce the impact of ADB.

Keywords: tree pathogen, tree disease, forest dynamics, ash dieback, chalara, prior growth rates, species mingling, size dominance, basal area of larger trees, tree diameter

1. INTRODUCTION

Ash dieback (ADB) disease, caused by the ascomycete fungus *Hymenoscyphus fraxineus*, has plagued European woodlands for nearly three decades. It has spread rapidly from East to West across the continent causing a major impact on ash populations and large areas of ash-dominated woodlands. In Europe, ADB was first recognised in Poland in the early 1990s (Kowalski, 2006) and was positively identified as arriving in Great Britain by 2012, since when it has infected populations of European ash (*Fraxinus excelsior*) across most of the UK (British Ecological Society, 2012; Pautasso et al., 2013; Stocks, Buggs & Lee, 2017). There have been many location- and country-specific reports of ADB-linked ash mortality from across Europe. However, predicting eventual mortality rates in mature ash trees is difficult due to the slow progression of the disease. Therefore, Coker et al. (2019) carried out a meta-analysis of published studies, together with a time-dependent model, to estimate longer-term mortality, leading to a pan-European prediction (with wide confidence intervals) of approximately 60% average cumulative mortality in natural woodland. However, plantation trials of young trees have shown that only 1-5% of the populations are genetically tolerant of ADB (e.g. Kjær et al., 2012; Stocks et al. 2017). Nevertheless, it is likely that ADB will have a lasting impact on the 953 animal and plant species associated with *F. excelsior* (Mitchell et al., 2014). ADB is one of the most researched topics in recent European woodland ecological literature, yet half of the studies involved laboratory-based experiments rather than *in situ* observations (Bowler, 2019). At present there is no effective silvicultural or other management response to slow the spread of the disease, once it has arrived in a region (Skovsgaard et al., 2017). Therefore, the primary focus has been on the long-term strategy of tree selection and breeding for resistance as the basis for restoration of ash populations (McKinney et al., 2014).

The disease induces symptoms of leaf wilting, dieback of twigs in the crown, and necrotic lesions in young shoots, bark, and leaf petioles. The clearest visible symptoms are epicormic sprouting on the trunk and branches (Enderle et al., 2018). Ascospores develop in the apothecia of leaf rachises

after they fall during the autumn and winter, and the following spring and summer they are released and dispersed by wind (Timmermann et al., 2011; Gross et al., 2014; Timmermann et al., 2017), leading to new infections and continuation of the cycle (Nemesio-Gorriz et al., 2019). This suggests that proximity to an infected tree will influence the probability and severity of infection. Inoculum density decreases rapidly up to 50 m from infected trees (Chandelier et al. 2014; Grosdidier et al., 2018), however it is estimated that the mean dispersal distance of ascospores is between 0.2 and 2.6 km, depending on the scale and dispersal kernel (statistical distribution of distances) fitted (Grosdidier et al., 2018).

The level of disease in the population of ash within a woodland is positively associated with various site factors, including air humidity and temperature, topography, occurrence and dimensions of watercourses, soil type and moisture (Klesse et al., 2021; Grosdidier et al., 2020; Chumanová et al., 2019; Erfmeier et al., 2019; Havrdová et al., 2017; Skovsgaard et al., 2017). Woodland structural and compositional factors may have an influence on ADB, including local tree density, light levels and tree species mixtures (Chumanová et al., 2019; Erfmeier et al., 2019). Furthermore, research has suggested that individual tree metrics may be correlated with ADB. Larger diameter trees, for example, have been found to display milder symptoms with a slower progression of ADB in the crown (Enderle, Stenlid & Vasaitis, 2019; Skovsgaard et al., 2010; Lenz et al., 2016; Marçais et al., 2016; Queloz, 2016; Havrdová et al., 2017). Previous studies also indicate that smaller and slower-growing trees are more susceptible to ADB and have higher mortality rates than larger, faster-growing individuals (Klesse et al., 2021; Klesse et al., 2020; Enderle, Stenlid & Vasaitis, 2019; Enderle et al., 2018; Marçais et al., 2017).

Recent research on the landscape epidemiology of ADB in northern France concluded that *F. excelsior* trees in isolated agricultural settings were less affected by the disease than those within forests (Grosdidier et al., 2020). This can be attributed to differences in microclimate, with higher crown temperatures in isolated trees that may restrict pathogen development, and/or to lower host density (as found in a grassland biodiversity experiment by Mitchell et al., 2002). A previous large-

scale study of ash forests in the Czech Republic also suggested that higher tree density and the proximity of certain tree species (such as *Quercus robur* and *Fagus sylvatica*), together with proximity to the nearest ash stand, as well as physical site environmental factors, can worsen the impact of the disease (Havrdová et al., 2016; Havrdová et al., 2017). Similarly, a nationwide study in Switzerland found higher mortality probability in stands with humid microclimate and high abundance of ash (Klesse et al., 2021). Thus, as well as the severity of ADB being linked to forest microclimate, proximity and density of infected ash hosts has a major influence on the rate of spore arrival on a susceptible tree.

The present study sought to determine the impact of a range of site environment, previous and present tree condition and near neighbourhood factors on the severity of ADB in a population of *F. excelsior* trees. The specific questions were: (1) is the severity of ADB greater with increasing tree density in the immediate neighbourhood of the focal tree; (2) is the severity of ADB less in trees that had a greater prior growth rate; (3) is the severity of ADB less in trees that had a greater crown dominance over their immediate neighbourhood; (4) is the severity of ADB less in trees whose neighbourhood is more dominated by heterospecific trees?

To answer these questions, we carried out a study during the early-mid stages of a developing ADB epidemic at Lady Park Wood, Monmouthshire, Wales, which has a well-established ash population in near natural growing conditions – most of the woodland has been left unmanaged for more than 70 years – as well as records of individual trees in permanent sample plots since 1945.

2.MATERIALS AND METHODS

2.1 STUDY SITE

The study site, Lady Park Wood, is a 36-hectare ancient woodland nature reserve containing 33 native tree and shrub species, dominated by *Tilia platyphyllos*, *Tilia cordata*, *Fagus sylvatica*, *Fraxinus excelsior*, *Betula* spp., *Quercus petraea*, *Ulmus glabra* and *Taxus baccata*. The soil across the woodland is heterogenous; its span of pH is one of the widest ranges in a single British woodland – from 7.9 to 3.8 (Peterken & Mountford, 2017) despite limestone being the dominant bedrock. Soil pH was measured in 288 samples over 72 evenly-distributed 200 m^2 plots (Peterken & Mountford, 2017), which we subsequently mapped onto the tree sample sub-plots described below. GPS altitude readings were taken in each sub-plot and used to calculate its mean slope gradient angle.

The long history of monitoring at the site provides rare longitudinal records from repeated censuses of all trees in ten long thin permanent sample plots, termed “transects”. All are 19.8 m wide and oriented parallel with the slope, but they vary in length from 150 m to 500 m (Figure 1). The transects have historically been categorised and sub-divided depending on when there was last human-caused disturbance, e.g. coppicing or thinning, and also by topographic position or dominant soil type. In Figure 1 and Table 1 we have sought to clarify the classification of these zones within the site, which define the non-overlapping ”stand types” analysed in this study.

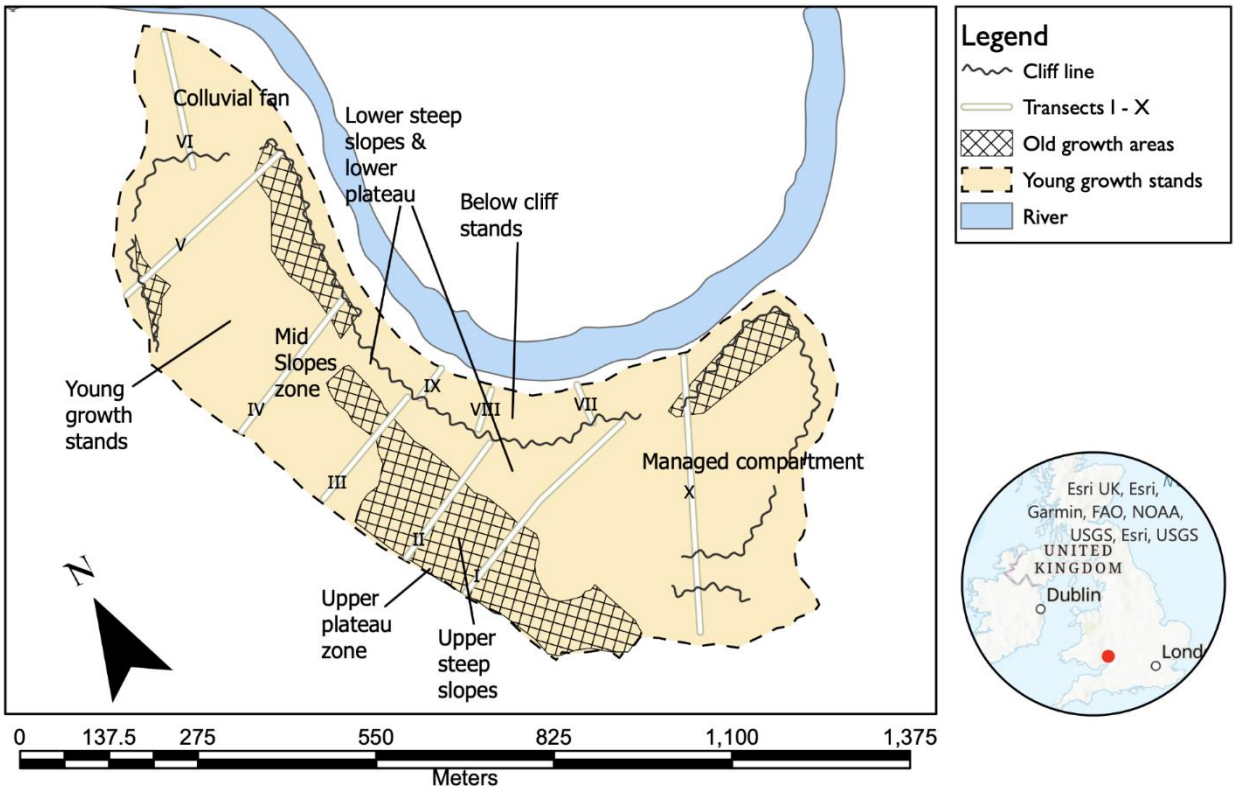

FIGURE 1. Map of Lady Park Wood, Monmouthshire, Wales, with the geographical location shown in the inset map. Stands in the unshaded areas ("young growth") were felled in 1942-3, leaving a shelterwood of larger individuals; the shaded areas ("old growth") were last coppiced ca. 150 years ago. Transects VII, VIII and IX occupy a separate topographic position with outcropping limestone and steep slopes: the "below cliff" stand, which is ecologically distinctive as the ground is much steeper, some felling took place in the early 1940s, and the relative density of *F. excelsior* and *Ulmus glabra* is higher than in the other stands. Transects I-VI were laid out and first recorded in 1944, VII-IX in 1955, and X in 1984. The majority of transect X is in stands thinned in 1984 and 1994, the "managed compartment", but there is some old growth at the cliff end and a small section of young growth at the top of the slope. The "colluvial fan" in the northern section of the wood is sampled by the lower two-thirds of Transect VI. Also shown are topographical zones, which differ in soil type and slope gradient, such as 'mid slopes', 'lower steep slopes' and 'upper plateau'.

TABLE 1. Distribution of the number of 30.5-m (100-ft) length transect sections amongst topographic and management history stand types in each of the ten transects. Each section has an area of 604 m^2. There is no overlap between the stand types

Transect	Old growth (OG)	Young growth (YG)	Colluvial fan (CF)	Below cliff (BC)	Managed compartment (MC)	Total number
I	5	5	-	-	-	10
II	5	2	-	-	-	7
III	2	5	-	-	-	7
IV	3	7	-	-	-	10
V	4	7	-	-	-	11
VI	-	2	4	-	-	6
VII	-	-	-	3	-	3
VIII	-	-	-	4	-	4
IX	-	-	-	3	-	3
X	2	-	-	1	12	15
Total number	**21**	**28**	**4**	**11**	**12**	**76**
Total area (m^2)	**12,680**	**16,910**	**2,420**	**6,640**	**7,250**	**45,900**

Nine of the transects (I-IX) are in woodland unmanaged for 78 years, which has been enclosed by a two-metre-high deer fence since 2007. There is considerable variation amongst and within them in both topographic position and past management. Above the limestone cliff that bisects the woodland into upper and lower sections, transects I-V each sample both "old growth" and "young growth" stands (Figure 1). The former was last coppiced in 1870 and the latter in 1942 just before the site became a reserve. Transect VI predominantly samples "young growth" woodland on well-drained soils of what is known as the "colluvial fan". Transects VII-IX are shorter being confined to the woodland below the limestone cliff. These "below cliff" stands are ecologically distinct being on steeply sloping ground and affected by some felling of *Tilia* spp. in 1942 for aircraft production; they have a higher relative density of *F. excelsior* and *Ulmus glabra* than in the other stands. Transect X was added in 1984 in an adjacent "managed" unfenced compartment, the majority of which has been thinned twice since then. Metrics of each stand type are given in Table 4.

Hand-drawn maps of the locations of the centre of each individual woody plant ≥1.3 m height in transects I-VI were recorded on a Cartesian coordinate grid by reference to transect edge markers with a regular 30.5-m spacing in 1977. Transects VII-X were similarly mapped in 1984-85. These records were updated and checked for accuracy at each successive enumeration of each transect, including in 2013 before ADB was first observed in the woodland and in anticipation of its arrival. For the present study these maps were scanned digitally using Esri ArcGIS Pro® 2.7.3 (2021) software onto Ordnance Survey digital maps and allocated their British National Grid coordinate values. The geographical location of the centre of each tree was normalised for slope. After the initial enumeration of each transect, all woody plants ≥ 1.3 m height (with no minimum diameter limit) in transects I-IX were identified to species, recorded as live or dead and measured for diameter at breast height (1.3 m, dbh) in 1955, 1977 and 1983, and in all ten transects in 1986, 1992, 2000, 2002, 2010, 2013 and 2018. In the case of the many multiple-stemmed coppice stools, an equivalent single diameter was assigned, calculated from the sum of their stem cross-sectional areas.

169

170 **2.2 TREE ATTRIBUTES**

171 A total of 464 *F. excelsior* trees across the ten permanent transects, representing all live individuals
172 ≥1.3 m height at the start of the study in 2019, were assessed for ADB symptoms in July and August
173 2019, and 381 during August 2020. The lower number in the second year is due to the increased
174 restriction on field-work due to risk assessment and restriction of available time under that
175 constraint. Therefore, our main statistical models were only applied to the more complete data set
176 recorded in 2019. We have used the 2020 data solely to assess the overall rate of progression of the
177 disease at the time of the study.

178 The severity of crown dieback was scored between 0 and 100% based on a visual estimation
179 of proportionate level of defoliation, similar to the assessment methods used in other studies of ADB
180 (Turczanksi, 2020; Grosdidier et al., 2020; Lenz et al., 2012). Two observers surveyed each focal tree
181 according to an agreed scale of crown defoliation in scoring classes of 0-10%, 10-20%, 20-30%, 30-
182 40%, 40-50%, 50-60%, 60-70%, 70-80%, 80-90%, 90-100%, with their assessments calibrated at
183 regular intervals against photographs of previously agreed percentage defoliation scores to ensure
184 scoring did not drift over the study. Independent scoring of the same tree by each of the observers
185 was conducted periodically to guard against observer bias and the scoring of the transects was
186 carried out in random order to avoid confounding with topographic/stand type. Ash trees with a
187 score of 0% crown dieback and no trunk sprouting or other visible sign of infection were classified as
188 uninfected.

189 Annual mortality rate (AMR) of ash, as a simple indicator of change from before to after the
190 onset of ADB in the study woodland, was calculated using the formula of Sheil et al. (1995): AMR = 1
191 – $(N_1/N_0)^{1/t}$, where N is the number of trees alive at each census and t is the number of years
192 between census 0 and census 1. Two periods of recorded prior growth rates were selected: 1977 to
193 2013, and 2000-2002 to 2013. Basal area of each tree was also calculated from the dbh
194 measurements as an explanatory variable in its own right for focal ash trees, but also to calculate

further explanatory variables, such as the total basal area of the stand. Basal area of larger trees (bal), an indicator of the level of competition for light on the focal tree at the stand level (Pommerening & Grabarnik, 2019; Wykoff, 1990), was calculated as the total basal area of all trees larger or equal to the basal area of the focal tree *i* in the same sub-plot at a particular time *t* (Table 2, formula 5). By "sub-plot" here we mean the regular subdivisions of the transect plots permanently marked by stakes at 400-ft (121.9-m) intervals down the slope, which were used for ease and accuracy of the successive enumerations of the transects but were also, it transpired during our study, the most ecologically appropriate for near-neighbour spatial analysis. The size of each sub-plot of the transects was 19.8 m x 121.9 m (2414 m^2) and they were arranged so that each lay entirely within either the "old growth" or "young growth" stands". An alternative measure of a focal tree's crown dominance relative to its neighbours was provided by the recording, in previous enumerations, of each tree's crown position in four categories: ground, understorey, sub-canopy, and canopy.

2.3 SPATIAL ANALYSIS

Spatial point-process methods were used to compute the Euclidean distances between nearest-neighbour points within each 2414 m^2 sub-plot (as illustrated in Figure 2). The 'spatstat' package in R was used to estimate near neighbour summary statistics (NNSS). Using 'spatstat', a number of established individual-tree neighbourhood indices were calculated (Baddeley, Rubak & Turner, 2015; Illian et al., 2008; Pommerening & Grabarnik, 2019) for use as explanatory variables, as outlined below. We used the minus-sampling "NN1" nearest neighbour edge-correction method outlined by Pommerening & Grabarnik (2019), in turn based on Hanisch (1984), for all these NNSS.

(i) Species mingling (mi) and weighted species mingling (wmi)

Both species mingling (mi) and richness-weighted species mingling (wmi) are spatially-explicit diversity indices. Species mingling (mi) is a calculated value between zero and one representing the

221 proportion of heterospecific (rather than conspecific) trees in the near neighbourhood of the focal
222 tree (Table 2, formula 1). So, if there are four neighbours counted and three are heterospecific, the
223 focal tree is given a species mingling value of 0.75. The total number of nearest neighbours (*k*) can
224 be varied according to the ecological context. We used a version of the formula which incorporates
225 weighting by the number of species in the *k* nearest neighbours, known as "richness-weighted
226 species mingling" (wmi) (Hui et al., 2011), with the weighting effect limited by the number of species
227 present in the focal tree's sub-plot (which sets the maximum possible number of species in *k* + 1
228 trees at that location) (Wang et al. 2021) (Table 2, formula 2). The wmi index is thus a more
229 sophisticated version of the mingling index, which encompasses the component of species richness
230 in a tree's heterospecific near neighbourhood, producing a greater variation in index values between
231 trees. However, to test the use of wmi for assessing the dominance of ash trees' neighbourhoods by
232 heterospecific trees, we examined the linear correlation of wmi with mi for the 464 ash trees
233 included in the study; the Pearson correlation co-efficient (*r*) was 0.89 giving us full confidence in
234 selecting wmi for this purpose.
235
236 *(ii) Size dominance (ui)*

237 The size dominance index (ui) measures the size of a focal tree relative to its *k* nearest neighbours
238 (Table 2, formula 3). We used stem diameter (dbh) to describe size, but other size characteristics are
239 also possible. The calculation of this index is similar to that of the species mingling index, with a value
240 between zero and one, and the potential to vary *k* (Hui et al., 1998; Aguirre et al., 2003; Pommerening
241 & Grabarnik, 2019).
242
243 *(iii) Local tree density (λ)*

244 Local tree density around a focal tree (λ) was calculated using a kernel smoothing function in R
245 (Baddeley, Rubak & Turner, 2015). It was originated by Diggle (1985) as "a method for estimating the

246 local intensity" as a point process, and it includes edge correction within the formula (Table 2, formula
247 4).

248

249

250

251

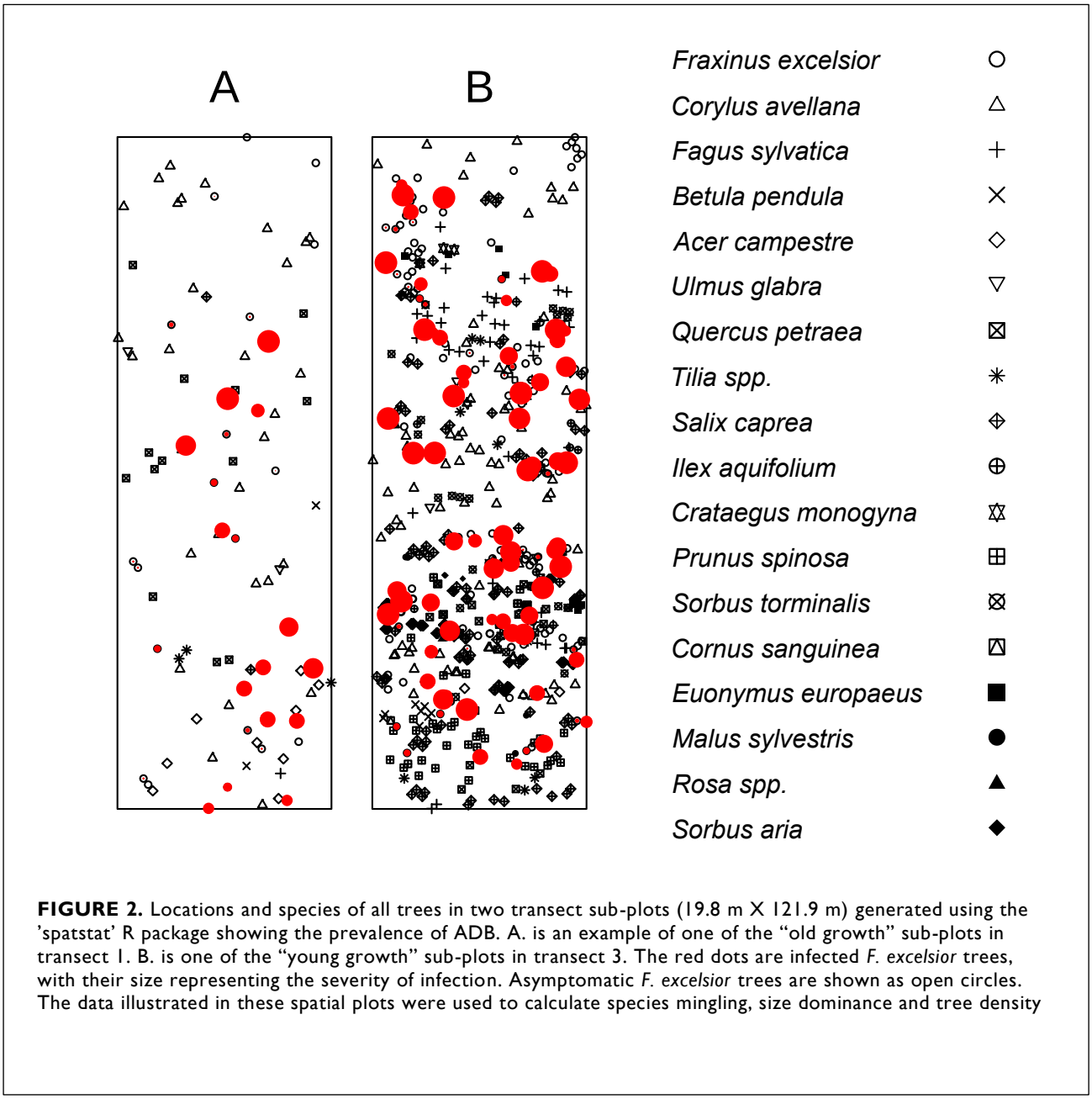

FIGURE 2. Locations and species of all trees in two transect sub-plots (19.8 m X 121.9 m) generated using the 'spatstat' R package showing the prevalence of ADB. A. is an example of one of the "old growth" sub-plots in transect 1. B. is one of the "young growth" sub-plots in transect 3. The red dots are infected *F. excelsior* trees, with their size representing the severity of infection. Asymptomatic *F. excelsior* trees are shown as open circles. The data illustrated in these spatial plots were used to calculate species mingling, size dominance and tree density

252

253 **TABLE 2**. Key formulae used to calculate the indices. *k* in all equations relates to the total number of nearest
254 neighbour trees considered in the formulae

255

Equation	Variable name	Variable category	Formula	NNSS definition
Near neighbourhood summary statistics (NNSS) formulae				
(1)	Species mingling (Gadow, 1993)	Species	$M_i = \frac{1}{k}\sum_{j=1}^{k} \mathbf{1}(species_i \neq species_j)$	$M_i \in [0, 1]$
(2)	Weighted species mingling (Hui et al., 2011; Wang et al., 2021)	Species	$M_i' = \frac{1}{k \cdot c}\sum_{j=1}^{k} \mathbf{1}(species_i \neq species_j) \cdot s_i$	s_i is species richness among *k* nearest neighbours of an including tree *i*; *c* = min(*S*, *k* + 1), where *S* is total species richness of forest stand
(3)	Size dominance (Hui et al., 1998; Aguirre et al., 2003)	Size	$U_i = \frac{1}{k}\sum_{j=1}^{k} \mathbf{1}(m_i > m_j)$	$U_i \in [0, 1]$
(4)	Local density (Diggle, 1985; Baddeley, Rubak & Turner 2015)	Density	$\hat{\lambda}_t(x) = \left\{\sum_{i=1}^{n} \delta_t(x - x_i)\right\}/p_t(x)$	$\hat{\lambda}_t$ = local intensity of focal trees $x_i, \delta(x)$ = kernel function, and $p_t(x)$ = end correction
Focal tree attributes formulae				
(5)	Basal area of trees > focal tree (Wykoff 1990; Pommerening & Grabarnik, 2019)	Size	$BAL_i(t) = G(t) \cdot (1 - p_i(t))$ with $p_i(t) = \frac{1}{G(t)}\sum_{\leq g_i(t)} g_i(t)$	Where *i* is a given tree at time *t*, basal area percentile is $p_i(t)$ of tree i denoting relative dominance, where *G*(*t*) is basal area ha^{-1} of forest stand at time *t*.
(6)	Basal area of tree (Gadow et al., 2021)	Size	$BA = \frac{\pi}{4} \cdot \sum_{i=1}^{n} dbh_i^2$ in cm^2 $BA = \frac{\pi}{40000} \cdot \sum_{i=1}^{n} dbh_i^2$ in m^2	*dbh* is diameter at breast height or 1.3 m.
Stand attributes formulae				
(7)	Basal area of forest stand (Pommerening & Grabarnik, 2019)	Size	$G = \frac{\sum_{i=1}^{n} g_i}{A}$	g_i is basal area of tree *i* in m^2, *N* is number of trees in stand, *A* is area of sample plot in ha

256

2.4 STATISTICAL ANALYSIS

The complex dataset of Lady Park Wood is derived from a range of historical and primary sources, as described above, which do not always overlap precisely and as such cannot be coerced into a single overarching statistical model. We have therefore categorised the potential predictor variables into two groups, which we have termed as 'non-spatial', dominated by edaphic and context-related variables, and by spatially explicit point-process statistical characteristics (Table 3). Variables that exist in both categories did not require post-processing in that they remain true to their original sources and coincidentally provide a useful bridge between the two groups. The historical sampling strategy was based on dividing the site into several different stand types and topographical zones. Our statistical methods were selected knowing that the sampling and methods had all the hallmarks of being nested and hierarchical (Wang et al., 2019). We used a model averaging approach (Dormann et al. 2018).

Prior to the modelling we investigated the most plausible distribution of our response variable (adb19) using the 'fitdistrplus' package, identifying a beta distribution as the most appropriate family for the models (Supporting Information; Zuur et al., 2009; Delignette-Muller et al., 2015). For selection of the predictor variables to include in the models, we assessed likelihood of collinearity amongst our full set of variables using Pearson's correlation. Where variable pairs were strongly correlated variables (> 0.7), only one was retained. We then identified variables that could not logically co-occur as predictors (due to legacy methods and/or variables being derivatives of each other). An example of inappropriate or at the very least uninterpretable inference might result from modelling of species mingling at more than one of 4, 5 and 6 nearest-neighbour tree ranges. Where pairs could not be precluded due to collinearity, a selection criterion for one of these pairs was applied using the lowest Akaike information criterion (adjusted for small sample size AICc) using the 'AICcmodavg' package (Mazerolle & Mazerolle, 2017). This process reduced the possible predictor variables in the non-spatial

set to seven, with 128 model permutations, and in the spatial set to six variables, with 64 model permutations.

For the model averaging stage of our procedure, we started with an initial 'global model' for each of the non-spatial and spatial models (formulae shown in the Supplementary Information). We used sampling 'transect' number (1-10) as a random effect and visually checked residuals for performance and comparison against the null model (Zuur et al., 2009). From the 128 non-spatial and 64 spatial model permutations we retained what are often defined as the 'top models' for each using the 'MuMIn' package (Bartoń, 2022) based on delta AICc < 2, as scores between 0 and 2 can be broadly considered equivalent despite potentially different combinations of predictors (Wagenmakers & Farrell, 2004; Burnham et al., 2011). All seven predictor variables were present in the non-spatial top models but one (ui6) was absent from the spatial top models (retaining the other five). These sets were then averaged and explored. To assess the effect of selecting the weighted mingling index (wmi) rather than the basic species mingling index (mi) a sensitivity analysis was carried out of the effect on the top models of switching from wmi to mi. All the statistical analyses were conducted in the R programming language and R Studio (R Core Team, 2021). A full description of the procedures for selection of beta distribution, variable elimination, model selection and the top models are shown in the Supplementary Information.

TABLE 3. List of response and predictor variables obtained from Lady Park Wood showing their potential for inclusion in non-spatial and spatial models. Log relative growth rate – short time period (rgr-s) data are not available for the managed compartment only due to lack of site access during 2000-2002. Formal definitions of the point process statistics are provided in Table 2

	Description	Non-spatial model	Spatial model
Epidemiological (response) variable			
adb19	Disease score in 2019 (% converted to 0-1 scale for beta distribution)	•	•
Site / edaphic /focal tree attribute predictors			
stand type	Old growth (OG), young growth (YG), below cliff (BC), colluvial fan (CF), managed compartment (MC) with thinned sub-compartments MC1 and MC2	•	•
transect	Transect number	•	•
pH	Soil pH	•	
gradient	Slope gradient (degrees)	•	
ash density	Density of *F. excelsior* trees in the sub-plot	•	
dbh77	Focal tree 1977 diameter at breast height (cm)	•	
dbh02	Focal tree 2000-2 diameter at breast height (cm)	•	

dbh13	Focal tree 2013 diameter at breast height (cm)	•	•
can19	Focal tree canopy score in 2019	•	
rgr-l	Focal tree log relative growth rate – long time period (1977 to 2013)	•	
rgr-s	Focal tree log relative growth rate – short time period (2000-2002 to 2013)	•	
Point process statistics predictors			
wmi4	Weighted species mingling (*k*=4)		•
wmi5	Weighted species mingling (*k*=5)		•
wmi6	Weighted species mingling (*k*=6)		•
ui4	Size dominance index (*k*=4)		•
ui5	Size dominance (*k*=5)		•
ui6	Size dominance (*k*=6)		•
ba	Basal area		•
bal	Basal area of larger trees in sub-plot		•
lambda	Local tree density		•

3. RESULTS

3.1 SUMMARY STATISTICS

The annual rate of mortality (AMR) of ash trees increased greatly since ADB was first recorded in the woodland in 2013. In the young-growth stands, from an initial population of 376, AMR was 0.1% during 1992-2013 and 1.4% (of 368 trees) during 2013-2019, and in the old-growth stands AMR was 0.4% (of 107 trees) and 1.8% (of 98 trees) in the two periods, respectively. All other stand types also showed a marked increase in AMR since 2013.

317 **TABLE 4.** Tree attributes by stand type in Lady Park Wood in 2019, including absolute values for trees of all
318 species and all ash trees, relative values for ash and severity of ADB

Stand type	All trees density (trees ha^{-1})	Ash tree density (trees ha^{-1})	Ash tree relative density (% per plot)	All trees basal area (m^2 ha^{-1})	Ash basal area (m^2 ha^{-1})	Ash relative basal area (% per plot)	All trees dbh (mean cm)	Ash dbh (mean cm)	% Ash infected in 2019	Mean ADB severity in 2019 (%)
Old growth	611	92	15%	37.2	8.3	22.4%	20.1	30.3	87%	40%
Young growth	1,343	236	18%	28.4	10.6	23.0%	10.9	13.9	85%	47%
Colluvial fan	1,258	100	8%	19.1	6.6	34.5%	8.4	22.6	95%	74%
Below cliff	616	70	11%	24.0	7.9	32.7%	14.7	29.3	89%	71%
Managed compartment	1,365	190	14%	19.3	6.8	14.3%	16.2	18.7	60%	25%
Mean	*1039*	*138*	*13%*	*25.6*	*8.0*	*25.4%*	*14.1*	*23.0*	*83%*	*51%*

319

320 Across the woodland the proportion of all recorded ash trees that were infected with ADB by 2019
321 was 81% (the mean of the values per stand type was 83%, Table 4). This had increased to 95% by 2020.
322 There was also a marked increase in the proportion of recorded ash trees with > 80% crown dieback
323 from 24.5% in 2019 to 41% in 2020. Ash trees that had a below-canopy crown position in 2013 had a
324 markedly higher severity of ADB in 2019 and to a lesser extent in 2020 than those with a canopy or
325 sub-canopy crown position (Figure 3). The proportion of ash trees infected and the severity of ADB
326 were greatest in the stands on the colluvial fan and below the cliff, which are adjacent to a wide river
327 (Figure 1) and have moister soils (Peterken & Mountford, 2017) and where ash accounts for the
328 highest proportion of the total basal area (Table 4). In contrast, both the proportion of infected ash
329 trees and severity of infection were notably lower in the managed compartment (in which ash
330 accounts for the lowest proportion of the total basal area and where there has been recent thinning
331 of trees) than in all the unmanaged compartments (Table 4). However, no consistent associations were
332 found, at the whole stand level, between the incidence of ADB infection and tree density (of all species
333 and of the absolute and relative density of ash specifically).

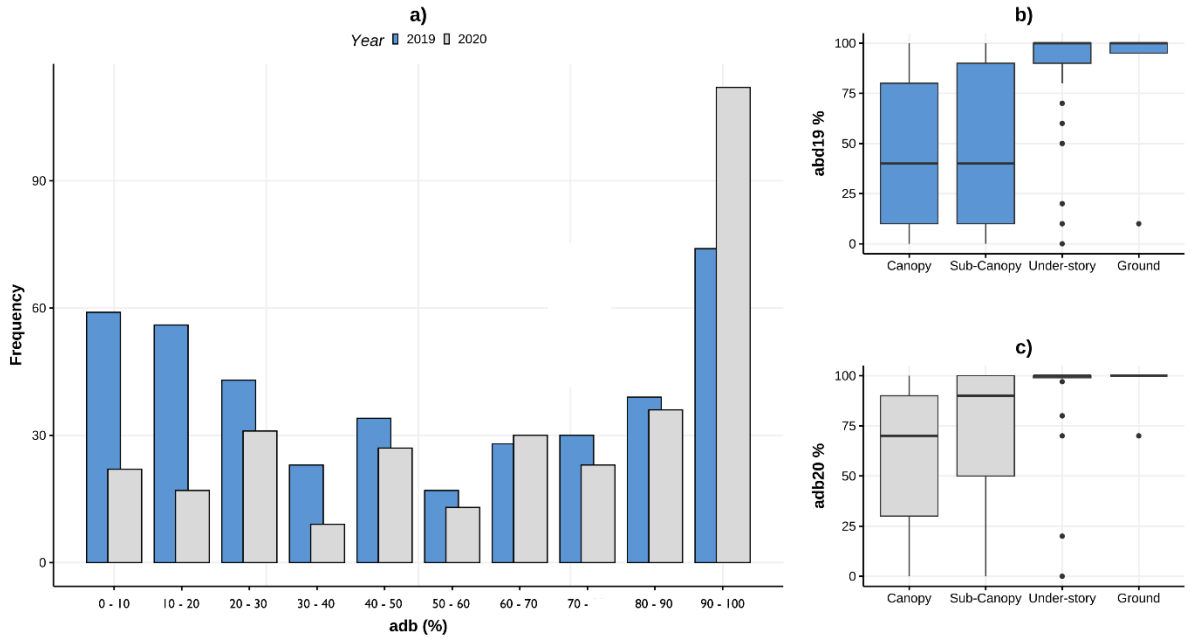

334

335

FIGURE 3. Severity of ADB (level of crown defoliation of ash trees): (a) across the whole woodland in 2019 and 2020 shown as frequency of the number of trees scored in each 10% class of defoliation; (b) box-and-whisker plot of ADB severity in the section of the forest with the greatest density of ash trees, the young growth stands, for trees with each of four crown positions in 2019 and (c) 2020. Trees with crowns in the canopy and sub-canopy are clearly less affected than those in the understorey and near the ground. Dieback severity increased in canopy and sub-canopy trees between 2019 and 2020

336

337 ### 3.2 NON-SPATIAL MODELLING

338 Results from the model selection procedure are provided in full in the Supporting
339 Information. The resulting models for the prediction of ADB in 2019 by the non-spatial
340 predictors outlined in Tables 2 and 3 included stand type and six other variables that made
341 an independent contribution to the variation between trees in their severity of ADB (Figure
342 4, Table 5). There is strong evidence that greater ADB severity was associated with smaller
343 2013 diameter at breast height, lower relative growth rate (between 2000-2002 and 2013)
344 and lower soil pH. The severity of ADB was much less in the young growth and old growth
345 stand types than the below cliff and colluvial fan stand types. It was only very weakly
346 associated with longer-term past relative growth rate, density of ash trees in the same sub-
347 plot or slope gradient.

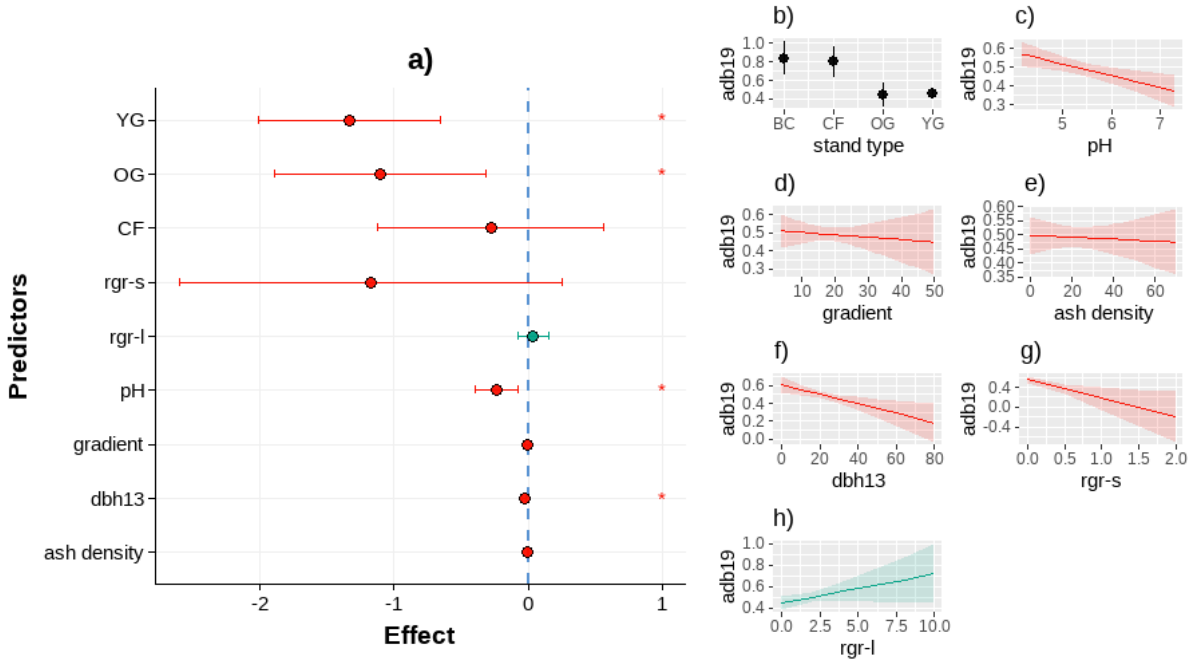

348

349 **FIGURE 4.** Non-spatial model a) Effect (model average coefficient) of non-spatial predictors on adb19 severity. Single
350 effect plots of the association of adb19 severity with each retained variable: b) stand type, c) pH, d) gradient, e) ash density,
351 f) dbh13, g) rgr-s and h) rgr-l. Variable abbreviations are defined in Table 3. All panels include 95% confidence intervals
352 coloured red or green for negative or positive average effects respectively

353

354

355

TABLE 5. Non-spatial variables predicting the severity of ash dieback in 2019. Estimated regression parameters, standard errors (SE), *z*-values, *p*-values and confidence intervals (CI) for model averaging and composite GLMMs of non-spatial variables selected via the procedure outlined in section 2.4 and models presented in Supporting Information Table S 3. Variable abbreviations are defined in Table 3

Variable	Estimate	SE	Adjusted SE	z value	*Pr*(>|*z*|)	CI lower	CI upper
(intercept)	3.260	0.717	0.720	4.527	< 0.01	1.849	4.672
YG	-1.336	0.346	0.347	3.847	< 0.01	-2.017	-0.655
OG	-1.105	0.403	0.404	2.729	< 0.01	-1.898	-0.311
CF	-0.278	0.430	0.432	0.644	0.519	-1.125	0.568
pH	-0.232	0.081	0.081	2.835	< 0.01	-0.393	-0.071
gradient	-0.004	0.009	0.009	0.533	0.593	-0.022	0.012
ash density	-0.0007	0.002	0.002	0.291	0.770	-0.005	0.004
dbh13	-0.026	0.007	0.007	3.736	< 0.01	-0.040	-0.012
rgr-s	-1.174	0.729	0.730	1.606	0.108	-2.606	0.258
rgr-l	0.037	0.058	0.058	0.636	0.524	-0.077	0.152

3.4 SPATIAL MODELLING

The models resulting from the selection procedure (see Supporting Information) for the prediction of ADB in 2019 by the spatial predictors outlined in Tables 1, 2 and 3 included stand type and four other variables that made an independent contribution to the variation between trees in their severity of ADB (Figure 5, Table 6). Greater ADB severity was strongly associated with greater weighted species mingling (i.e., a lower proportion of conspecific trees among the six nearest neighbours of the focal trees weighted by their species richness). The sensitivity analysis showed that use of the basic species mingling index (mi6) in place of the weighted index (wmi6) had a minimal effect on the model results (Tables S4 and S5 in Supplementary Information). It was also significantly associated with smaller 2013 diameter at breast height (Figure 5, Table 6). The severity of ADB was much less in the young growth, old growth and especially in the managed compartment stand types than in the below cliff and colluvial fan stand types. It was only very weakly associated with local tree density or basal area of larger trees, and was not independently associated with size dominance of the focal tree.

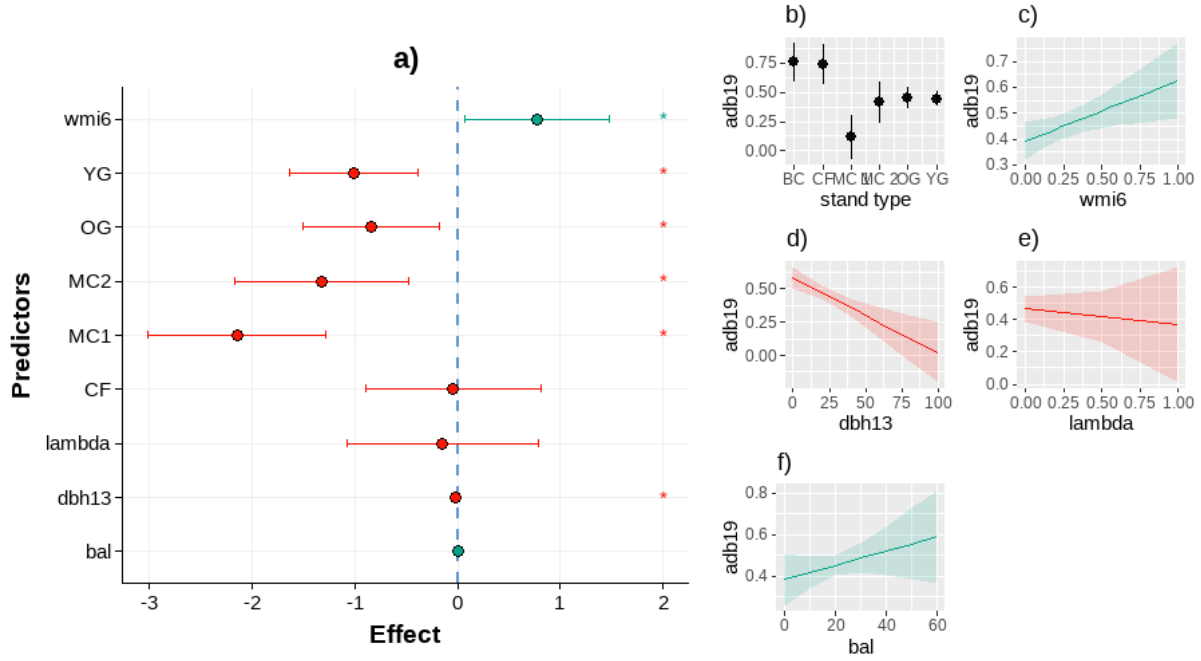

FIGURE 5. Spatial model a) Effect (model average coefficient) of spatial predictors on adb19 severity. Single effect plots of the association of adb19 severity with each retained variable: b) stand type, c) wmi6, d) dbh13, e) lambda and f) bal. Variable abbreviations are defined in Table 3. All panels include 95% confidence intervals coloured red or green for negative or positive average effects respectively

TABLE 6. Spatial variables predicting the severity of ash dieback in 2019. Estimated regression parameters, standard errors (SE), *z*-values, *p*-values and confidence intervals (CI) for model averaging and composite GLMMs of spatial variables selected via the procedure outlined in section 2.4 and models presented in Supporting Information Table S 4. Variable abbreviations are defined in Table 3

Variable	Estimate	SE	Adjusted SE	z value	*Pr*(>|*z*|)	CI lower	CI upper
(intercept)	1.157	0.386	0.387	2.988	< 0.01	0.398	1.916
YG	-1.005	0.318	0.319	3.151	< 0.01	-1.631	-0.380
OG	-0.839	0.337	0.337	2.486	0.012	-1.500	-0.178
CF	-0.041	0.431	0.432	0.096	0.923	-0.888	0.806
MC1	-2.147	0.439	0.440	4.881	< 0.01	-3.009	-1.285
MC2	-1.323	0.432	0.433	3.056	< 0.01	-2.172	-0.474
wmi6	0.777	0.357	0.358	2.169	0.030	0.075	1.480
dbh13	-0.023	0.006	0.006	3.830	< 0.01	-0.035	-0.011
lambda	-0.148	0.473	0.474	0.313	0.754	-1.078	0.781
bal	0.001	0.005	0.005	0.220	0.826	-0.009	0.011

4. DISCUSSION

The level of ADB reached at the early-mid stage of the epidemic in Lady Park Wood was clearly linked to site environment factors. The GLMM results showed that there was a very large and significant difference in severity of the disease amongst the stand types occupying different topographic positions and with different management histories within the woodland. The high incidence of disease in the colluvial fan and below-cliff sites are as expected from previous studies reporting greater infection in sites with moist soils (e.g., Muñoz et al., 2016; Havrdová et al., 2017; Skovsgaard et al., 2017), which is generally attributed to greater production of inoculum from litter and is associated with a greater occurrence of basal lesions (Marçais et al., 2016). Topographic and substrate factors may also influence crown dieback symptoms via their impact on rooting depth and drainage (Skovsgaard et al., 2017). Our observations of variation amongst the topographic zones indicate that trees on the lower slopes and upper steep slopes were much more severely affected than those on the intermediate mid-slopes (which have greater moisture retention during drought), and there is existing evidence of the importance of this moisture variation on tree ecophysiology at Lady Park Wood (Peterken & Mountford, 2017). Cavin et al. (2013) studied the long-term effects of drought events and found that they can lead to changes in the competition dynamics amongst the tree species' populations. Given that ash is known to be susceptible to drought (Zollner & Kölling, 1994; Berger et al., 2010; Dobrowolska et al., 2011; Drenkhan, Sander & Hanso, 2014) it is possible that trees on sites subject to greater variation in moisture availability have reduced resistance to ADB. The low incidence and significantly lower severity of ADB in the managed compartment that has been subject to recent thinning is also a striking result.

Our first question was derived from previous research that found a clear positive association between higher levels of ADB and dense, unthinned stands (Skovsgaard et al., 2017; Bakys, Vasaitis &

418 Skovsgaard, 2013), with lower levels amongst dispersed ash trees in an agricultural matrix than within
419 woodland at a landscape scale (Grosdidier et al., 2020). However, the results of the present study
420 showed no marked relationship between incidence or severity of ADB and the density of trees (of all
421 species) at the whole stand level or between severity of ADB and local tree density around individual
422 focal ash trees calculated using a kernel function (lambda), hence our answer to the first question is
423 'no'.

424 Site and neighbourhood effects could occur through either their influence on the rate of
425 transmission of ascospores or on the resistance to infection of ash trees mediated by their
426 physiological condition. It is unlikely that, at this stage of the epidemic, spatial variation (at stand and
427 individual tree scales) in the density of *H. fraxineus* ascospores is the primary cause of the variation in
428 ADB severity of individual trees recorded in the present study within an unfragmented closed-canopy
429 woodland. This finding is strongly supported by the GLMM result showing a lack of any meaningful
430 relationship between severity of ADB and the density of ash trees in the same sub-plot as the focal
431 tree. In 2019, two years after ADB was first recorded in this well-monitored site, overall, 81% of ash
432 trees were infected, and that had increased markedly to 95% by the following summer of 2020. It is
433 likely, therefore, that the density of dispersed ascospores across the site was already so high that
434 every susceptible ash tree was subject to a high inoculum load. ADB of a single tree produces millions
435 of tiny ascospores that disperse widely even in dry conditions (estimated mean dispersal distance 0.2-
436 2.6 km (Grosdidier et al., 2018)), though with a rapid decline in dispersed inoculum density up to 50
437 m from an infected host (Chandelier et al., 2014). In this context, the large differences in both infection
438 rate and, to an even greater extent, severity observed amongst the different stands in the study
439 woodland at this early-mid stage of the epidemic are notable, and the stands with the highest
440 percentage of trees infected and severity of ADB had only moderate or low absolute density and basal
441 area of ash trees (Table 4).

442 Our second question addressed the alternative mechanism explaining variation between ash
443 trees in their severity of ADB: that their resistance to or recovery from infection is mediated by their

444 physiological condition, for example, earlywood vessel size and slower growth feeding back and
445 amplifying crown dieback (Klesse et al., 2020; Skovsgaard et al. 2017). To assess this, it is a unique
446 strength of the present study that Lady Park Wood has a long record of the prior growth rates of
447 individual ash trees in permanent sample plots as a valuable indicator of their condition. This revealed
448 a strong negative association between severity of ADB and relative stem radial growth rates during
449 the 11 years immediately prior to the first observation of the disease in the woodland. This provides
450 robust evidence to answer yes to the second question: trees in a more vigorous condition had greater
451 resistance to the disease. This result is compatible with earlier studies based on less precise evidence
452 that showed a negative relationship between the severity of ADB and tree "vitality" in Scandinavia
453 (Bengtsson et al., 2021; Timmerman et al., 2017), and the conclusion of Skovsgaard et al. (2017) that
454 vigorous trees can better compensate for the effects of *H. fraxineus.* Previous studies have also shown
455 that tree height can be a significant strong predictor of lower rates of ADB defoliation (Erfmeier et al.,
456 2019), as well as individual tree vigour (Dobbertin, 2005), and our result that lower ADB severity is
457 significantly associated with larger diameter at breast height matches the findings of previous studies
458 (e.g., Klesse, 2021; Skovsgaard et al., 2010, Marçais et al., 2016; Enderle, Stenlid & Vasaitis 2019). It
459 may be that such a negative association between recorded severity of ADB and tree size at the earlier
460 stages of an epidemic may simply be a matter of time, with the infection taking longer to penetrate
461 all the vascular tissue of larger diameter individuals (Thomas, 2016; Erfmeier et al., 2019). Other
462 studies have suggested that in time ADB can infect ash trees of all sizes and ages (Pautasso et al.,
463 2013).

464 Tree growth rates integrate many factors, including genotype, site environment and (as the
465 basis for our third question) influence exerted by nearest neighbour trees, which may have differential
466 impacts on resistance to ADB. The evidence for the effect of site environment factors was reviewed
467 above. Our results provide only limited evidence that the lower the level of neighbour competition on
468 an ash tree, the lower its severity of ADB at this stage of the epidemic. We found a quantitative
469 indication (Figure 3) that taller ash trees with crowns scored as having canopy and sub-canopy crown

positions had much lower severity of ADB than those with crowns below the canopy, however this was not corroborated by the spatial GLMM model result showing no association of ADB severity with the basal area of larger trees. Therefore, our results only provide equivocal evidence for an answer of yes to the third question.

A striking result of the spatial GLMM was that the severity of ADB was significantly positively associated with a lower proportion of conspecific ash trees among the six nearest neighbour trees of a focal ash tree weighted by their species richness (as shown by the weighted species mingling index, and corroborated by both the strong correlation of this index with the basic species mingling index and the equivalence of the model results obtained with the basic index in the sensitivity analysis). The direction of this result was contrary to the expectation of the fourth question. Grossman et al. (2019), in a temperate forest, and Rutten et al. (2021) in a sub-tropical forest, also reported the occurrence of both positive and negative effects of a more species-diverse tree neighbourhood on the susceptibility to disease of individual tree species. Keesing et al. (2006) described a suite of mechanisms whereby species richness can either decrease or increase disease risk including the "dilution effect" where increased density of heterospecific neighbours reduces infection rates (Mitchell et al., 2002). Some other reported mechanisms can be excluded in the context of the present study as *H. fraxineus* is not known to have alternative host species amongst the flora of Lady Park Wood and animal vectors are not thought to be important in its transmission. Previous studies have indicated a distance component of other species mixture effects. Murrell & Law (2003) postulated that inter-species competition occurs at shorter distances than intra-species competition ("heteromyopia") and a reversal of tree interaction effects between shorter and longer distances has been demonstrated in various other contexts (Pommerening & Sanchez Meador, 2018). The evidence available from the present study does not allow the contradiction amongst these findings to be resolved and this stands out as a priority for future research. This will be important to provide a stronger mechanistic basis for the widely-held view that mixed-species stands, as opposed to

monocultures, have a reduced susceptibility to tree diseases (Pautasso et al., 2005), which has been supported by the results of a recent systematic review (Roberts et al. 2020).

There is evidence that the species identity of the near neighbours of ash trees can influence, either positively or negatively, the severity of their ADB specifically (Havrdová et al. 2017). Therefore, key to understanding the mechanisms of the species mingling result will be an analysis of the difference in effect of individual species of neighbouring tree present at Lady Park Wood. Some inference can be drawn from existing knowledge of the key species. In terms of above-ground competition from the abundant canopy species it is *F. sylvatica* and *Tilia* spp. that cast the densest shade (Ellenberg, 1988). The level of below-ground competition from different neighbouring species is likely to interact with site substrate properties. *Fagus sylvatica*, an abundant species in many areas of Lady Park Wood, is also highly competitive for below-ground resources, especially in certain soil layers (Pretzsch et al. 2010; Bolte, Kampf & Hilbrig, 2013). It is water demanding, however as a result its importance as a competitor may have been diminished due to its elevated mortality rate and the long-term reduction in its growth rates following the drought of 1976 (Cavin et al., 2013). The role of *F. sylvatica* trees as competitive neighbours is known to be complex: in old-growth forests high levels of conspecific above-ground competition (shading) on *F. sylvatica* trees were found to reduce or even reverse the negative effects of below-ground competition (Fichtner et al. 2015).

Instead of being a result of competition, neighbouring tree effects could be mediated by the influence of their leaf litter chemistry. For example, Havrdová et al. (2017) found that ADB severity was greater in ash trees where *F. sylvatica*, *Quercus* spp. and *Betula pendula* were present in their neighbourhood, and lower in the presence of *Abies* spp*., Pinus* spp. *and Acer* spp*.* They suggest that this could be explained by the interaction of different chemical and physical characteristics of the litter of different species, leading to different rates of leaf decomposition in species mixtures and a consequent effect on the degradation of ash petioles and thus ADB ascospore production.

It is therefore a priority for future research to test the relationship between severity of ADB and the species identity, as well as relative size, of neighbouring trees. Such evidence would indicate

the value of making greater use of NNSS based on species identity. Relative size of nearest neighbours is, however, likely to remain the dominant factor via its effect on the vigour of the focal tree (Pommerening & Sanchez Meador, 2018). Species identity is thus likely to be most important for dominant "monumental" individuals in influencing the composition and spatial structure of trees in their neighbourhood (Cholewińska et al. 2021).

The unique dataset provided by the permanent sample plots at Lady Park Wood has enabled a statistical modelling procedure that provides evidence of at least four significant effects on the severity of ADB of individual ash trees at this early-mid stage of the epidemic. The procedure narrowed the selection of potential predictor variables and indicates the potential for the untested factor of genotypic variation in resistance amongst individual ash trees (not linked to their prior growth rate) to account for a high proportion of variation in their severity of infection, as well as the inherently stochastic nature of the infection process. While this supports findings that there may be sufficient genetic variation within the ash population on which natural selection for greater disease resistance may act (Stener, 2018; Stocks et al., 2019), the notable increase in percentage of infected trees between the sixth and seventh years after first detection of the pathogen in Lady Park Wood (from 81% to 95%) reduces this optimism. Future monitoring will be crucial to determine what proportion of the ash trees have sufficient resistance to survive the infection and subsequently set seed.

The findings of our research have advanced those of previous studies (e.g., Grosdidier et al., 2020) by highlighting the influence of individual tree neighbourhood effects within mixed-species forests, as well as reinforcing at an intensive population scale the findings of Klesse et al. (2021) concerning a tree's previous relative growth rate as a separate effect from its size. They do not support growing ash in tree species mixtures as an effective measure to reduce the severity of ADB. However, they do indicate the potential contribution of silvicultural measures aimed at establishing species mingling patterns, and thinning targeted at reducing competition levels, based on the species of neighbouring trees as well as their relative size, in addition to genetic selection, all

targeted at increasing the vigour of ash trees in order to increase their resistance to subsequent ADB infection.

5. ACKNOWLEDGEMENTS

We thank Rolf Turner, Ege Rubak and Adrian Baddeley for technical advice on the use of their 'spatstat' R package, Owain Barton for advice on the statistical modelling, and James Walmsley, Mark Rayment, Andy Smith and Andrew Packwood of Bangor University for advice on collection and processing of data, and for advice on the original research proposal. We are grateful to Natural England and Forestry England for allowing access to Lady Park Wood, and all the various researchers and recorders of data over the past 75 years, particularly Eustace Jones, Alan Orange, Vanessa Williams and Edward Mountford. We thank four anonymous reviewers for their valuable comments.

6. AUTHORS' CONTRIBUTIONS

G.P. recorded the ash population in 2013-2015 in anticipation of ADB and was responsible with many others for accumulating the earlier records. D.C. and G.P. designed the study with J.H. D.C. collected most of the 2019/2020 data. D.C. processed and analysed the historic data and maps, did all the initial data analysis and led the writing of the manuscript. J.H. advised on data analysis and contributed to writing the manuscript. A.P. advised on the selection and use of point process statistics, wrote the corresponding R code and contributed to the methods section and analysis. P.L. carried out the statistical procedure and GLMM modelling, and redrafted corresponding parts of the manuscript. All authors contributed critically and edited the manuscript and gave final approval for publication.

7. DATA AVAILABILITY STATEMENT

All datasets are available at https://doi.org/10.5061/dryad.ngf1vhhxg.

8. ORCHID

David J. Cracknell https://orcid.org/0000-0002-2428-2335

George F. Peterken https://orcid.org/0000-0003-2187-1457

Arne Pommerening https://orcid.org/0000-0002-3441-2391

Peter J. Lawrence https://orcid.org/0000-0002-9809-0221

John R. Healey https://orcid.org/0000-0002-5398-2293

9. REFERENCES

Aguirre, O., Hui, G., Gadow, K., & Jimenez, J. (2003). An analysis of spatial forest structure using neighbourhood-based variables. *Forest Ecology and Management*, *183*, 137–145.

Baddeley, A., Rubak, E., & Turner, R. (2015). *Spatial Point Patterns: Methodology and Applications with R*. Taylor & Francis Group, Boca Ratan. https://doi.org/10.1201/b19708

Bakys, R., Vasaitis, R., & Skovsgaard, J. P. (2013). Patterns and severity of crown dieback in young even-aged stands of european ash (*Fraxinus excelsior* l.) in relation to stand density, bud flushing phenotype, and season. *Plant Protection Science*, *49*, 120–126. https://doi.org/10.17221/70/2012-pps

Bartoń, K. (2022). MuMIn: Multi-Model Inference (1.46.0). https://CRAN.R-project.org/package=MuMIn

Bengtsson, V., Stenström, A., Wheater, C. P., & Sandberg, K. (2021). The impact of ash dieback on veteran trees in Southwestern Sweden. *Baltic Forestry*, *27*, 558. https://doi.org/10.46490/BF558

Berger, R., Heydeck, P., Baumgart, A., & Roloff, A. (2010). Neue ergebnisse zum eschentriebsterben. *AFZ-Wald*, *65*, 18–21.

Bolte, A., Kampf, F., & Hilbrig, L. (2013). Space sequestration below ground in old-growth spruce-beech forests-signs for facilitation? *Frontiers in Plant Science, 4*, 322. https://doi.org/10.3389/fpls.2013.00322.

Bowler, A. (2019). Trends in research surrounding Chalara ash dieback (*Hymenoscyphus fraxineus*) between 1992 and 2019 - A systematic review*. MSc Dissertation.* Bangor University.

British Ecological Society. (2012). First occurrence of 'ash dieback' in Britain. Ecology and Policy Blog. http://www.britishecologicalsociety.org/first-occurrence-of-ash-dieback-in-britain/ (accessed 10th June 2023).

Burnham, K. P., Anderson, D. R. & Huyvaert, K. P. (2011). AIC model selection and multimodel inference in behavioral ecology: some background, observations, and comparisons. *Behavioral Ecology and Sociobiology*, 65, 23-35.

Cavin, L., Mountford, E. P., Peterken, G. F., & Jump, A. S. (2013). Extreme drought alters competitive dominance within and between tree species in a mixed forest stand. *Functional Ecology*, *27*, 1424–1435. https://doi.org/10.1111/1365-2435.12126

Chandelier, A., Helson, M., Dvorak, M., & Gischer, F. (2014). Detection and quantification of airborne inoculum of Hymenoscyphus pseudoalbidus using real-time PCR assays. *Plant Pathololog*y, *63*, 1296–1305.

Cholewińska, O., Keczyński, A., Kusińska, B., & Jaroszewicz, B. (2021). Species identity of large trees affects the composition and the spatial structure of adjacent trees. *Forests*, *12*, 1162. https://doi.org/10.3390/f12091162

Chumanová, E., Romportl, D., Havrdová, L., Zahradník, D., Pešková, V., & Černý, K. (2019). Predicting ash dieback severity and environmental suitability for the disease in forest stands. *Scandinavian Journal of Forest Research*, *34*, 254–266. https://doi.org/10.1080/02827581.2019.1584638

Coker, T. L. R., Rozsypálek, J., Edwards, A., Harwood, T. P., Butfoy, L., & Buggs, R. J. (2019). Estimating mortality rates of European ash (*Fraxinus excelsior*) under the ash dieback (*Hymenoscyphus fraxineus*) epidemic. *Plants People Planet, 1*, 48-58. https://doi.org/10.1002/ppp3.11

Delignette-Muller, M. L., Dutang, C., Pouillot, R., Denis, J. B., & Siberchicot, A. (2015). Package 'fitdistrplus'. *Journal of Statistical Software, 64*, 1-34.

Diggle, P.J. (1985). A kernel method for smoothing point process data. Journal of the Royal Statistical Society, Series C (Applied Statistics), *34*, 138–147.

Dobbertin, M. (2005). Tree Growth as Indicator of Tree Vitality and of Tree Reaction to Environmental Stress: A Review. *European Journal of Forest Research*, *124*, 319–333. http://dx.doi.org/10.1007/s10342-005-0085-3

Dobrowolska, D., Hein, S., Oosterbaan, A., Wagner, S., Clark, J., & Skovsgaard, J. P. (2011). A review of European ash (*Fraxinus excelsior* L.): Implications for silviculture. *Forestry*, *84*, 133–148. https://doi.org/10.1093/forestry/cpr001

Dormann, C. F., Calabrese, J. M., Guillera-Arroita, G., Matechou, E., Bahn, V., Bartoń, K., Beale, C. M., Ciuti, S., Elith, J., Gerstner, K., Guelat, J., Keil, P., Lahoz-Monfort, J. J., Pollock, L. J., Reineking, B., Roberts, D. R., Schröder, B., Thuiller, W., Warton, D. I., Wintle, B. A., Wood, S. N., Wüest, R. O. and Hartig, F. (2018). Model averaging in ecology: a review of Bayesian, information-theoretic, and tactical approaches for predictive inference. *Ecological Monographs, 88*, 485-504. https://doi.org/10.1002/ecm.1309

Drenkhan, R., Sander, H., & Hanso, M. (2014). Introduction of Mandshurian ash (Fraxinus mandshurica Rupr.) to Estonia: Is it related to the current epidemic on European ash (F. excelsior L.)? *European Journal of Forest Research*, *133*, 769–781.

Ellenberg, H. (1988). *Vegetation Ecology of Central Europe*. Cambridge University Press, Cambridge.

Enderle, R., Metzler, B., Riemer, U., & Kändler, G. (2018). Ash dieback on sample points of the national forest inventory in south-western Germany. *Forests*, *9*, 25. https://doi.org/10.3390/f9010025

Enderle, R., Stenlid, J., & Vasaitis, R. (2019). An overview of ash (*Fraxinus* spp.) and the ash dieback disease in Europe. *CAB Reviews, 14*, No. 025. https://doi.org/10.1079/PAVSNNR201914025

Erfmeier, A., Haldan, K. L., Beckmann, L. M., Behrens, M., Rotert, J., & Schrautzer, J. (2019). Ash dieback and its impact in near-natural forest remnants – a plant community-based inventory. *Frontiers in Plant Science*, *10*, 658. https://doi.org/10.3389/fpls.2019.00658

Fichtner, A., Forrester, D. I., Härdtle, W., Sturm, K., & Von Oheimb, G. (2015). Facilitative-competitive interactions in an old-growth forest: The importance of large-diameter trees as benefactors and stimulators for forest community assembly. *PLoS ONE*, *10*, e0120335. https://doi.org/10.1371/journal.pone.0120335

Gadow, K.V. (1993). Zur Bestandesbeschreibung in der Forsteinrichtung [New variables for describing stands of trees]. *Forst und Holz, 48*, 602–606.

Gadow, K.V., González, J.G.Á., Zhang, C., Pukkala, T., & Zhao, X. (2021). Sustaining Forest Ecosystems. Springer Nature.

Grosdidier, M., Ioos, R., Husson, C., Cael, O., Scordia, T., & Marçais, B. (2018). Tracking the invasion: dispersal of *Hymenoscyphus fraxineus* airborne inoculum at different scales. *FEMS Microbiology Ecology*, *94*, fiy049. https://doi.org/10.1093/femsec/fiy049

Grosdidier, M., Scordia, T., Ioos, R., & Marçais, B. (2020). Landscape epidemiology of ash dieback. *Journal of Ecology*, *108*, 1789–1799. https://doi.org/10.1111/1365-2745.13383

Gross, A., Holdenrieder, O., Pautasso, M., Queloz, V., & Sieber, T. N. (2014). *Hymenoscyphus pseudoalbidus*, the causal agent of European ash dieback. *Molecular Plant Pathology, 15*, 5–21. https://doi.org/10.1111/mpp.12073

Grossman, J.J., Cavender-Bares, J., Reich, P.B., Montgomery, R.A., & Hobbie, S.E. (2018). Neighbourhood diversity simultaneously increased and decreased susceptibility to contrasting herbivores in an early-stage forest diversity experiment. *Journal of Ecology, 107*, 1492-1505. https://doi.org/10.1111/1365-2745.13097

Hanisch, K. H. (1984). Some remarks on estimators of the distribution function of nearest neighbour distance in stationary spatial point processes. *Mathematische Operationsforschung und Statistik. Series Statistics, 15*, 409–412. https://doi.org/10.1080/02331888408801788.

Havrdová, L., Novotná, K., Zahradník, D., Buriánek, V., Pešková, V., Šrůtka, P., & Černý, K. (2016). Differences in susceptibility to ash dieback in Czech provenances of Fraxinus excelsior. *Forest Pathology*, *46*, 281–288. https://doi.org/10.1111/efp.12265

Havrdová, L., Zahradník, D., Romportl, D., Pešková, V., & Černý, K. (2017). Environmental and silvicultural characteristics influencing the extent of ash dieback in forest stands. *Baltic Forestry*, *23*, 168–182.

Hui, G., Zhao, X., Zhao, Z., & von Gadow, K. (2011). Evaluating tree species spatial diversity based on neighborhood relationships. *Forest Science*, *57*, 292–300. https://doi.org/10.1093/forestscience/57.4.292

Hui, Y., Albert, M., & Gadow, K. (1998). Diameter dominance as a parameter for simulating forest structure. *Forstwissenschaftliches Centralblatt*, *117*, 258–266.

Illian, J., Penttinen, A., Stoyan, H., & Stoyan, D. (2008). *Statistical Analysis and Modelling of Spatial Point Patterns*. John Wiley & Sons, Chichester. https://doi.org/10.1002/9780470725160

Keesing, F., Holt, R. D., & Ostfeld, R. S. (2006). Effects of species diversity on disease risk. *Ecology Letters*, *9*, 485–498. https://doi.org/10.1111/j.1461-0248.2006.00885.x

Kjær, E. D., McKinney, L. V., Nielsen, L. R., Hansen, L. N. & Hansen, J. K. (2012). Adaptive potential of ash (*Fraxinus excelsior*) populations against the novel emerging pathogen *Hymenoscyphus pseudoalbidus*. *Evolutionary Applications*, *5*, 219-228. https://doi.org/10.1111/j.1752-4571.2011.00222.x

Klesse, S., Abegg, M., Hopf, S. E., Gossner, M. M., Rigling, A., & Queloz, V. (2021). Spread and Severity of Ash Dieback in Switzerland – Tree Characteristics and Landscape Features Explain Varying Mortality Probability. *Frontiers in Forests and Global Change*, *4*, Article 645920. https://doi.org/10.3389/ffgc.2021.645920

Klesse, S., von Arx, G., Gossner, M. M., Hug, C., Rigling, A., and Queloz, V. (2020). Amplifying feedback loop between growth and wood anatomical characteristics of *Fraxinus excelsior* explains size-related susceptibility to ash dieback. *Tree Physiology, 41*, 683-696 https://doi.org/10.1093/treephys/tpaa091

Kowalski, T. (2006). Chalara fraxinea sp. nov. associated with dieback of ash (Fraxinus excelsior) in Poland. Forest Pathology, 36, 264–270. https://doi.org/10.1111/j.1439-0329.2006.00453.x

Lenz, H. D., Bartha, B., Straßer, L., & Lemme, H. (2016). Development of ash dieback in south-eastern Germany and increasing occurrence of secondary pathogens. *Forests, 7,* 41. https://doi.org/10.3390/f7020041

Lenz, H.D., Straßer, L., Baumann, M. & Baier, U. (2012). Boniturschlüssel zur Einstufung der Vitalität von Alteschen. *AFZ-DerWald, 67(3)*, 18–19.

713 Marçais, B., Husson, C., Caël, O., Dowkiw, A., Delahaye, L., Collet, C., et al. (2017). Estimation of ash
714 mortality induced by Hymenoscyphus fraxineus in France and Belgium. *Baltic Forestry, 23*, 159–
715 167.

716 Marçais, B., Husson, C., Godart, L., & Caël, O. (2016). Influence of site and stand factors on
717 *Hymenoscyphus fraxineus*-induced basal lesions. *Plant Pathology, 65,* 1452–1461.
718 https://doi.org/10.1111/ppa.12542

719 Mazerolle, M. J. & Mazerolle, M. M. J. (2017). Package 'AICcmodavg'. R package, 281.

720 McKinney, L.V., Nielsen, L.R., Collinge, D.B., Thomsen, I.M., Hansen, J.K., & Kjær, E.D. (2014). The ash
721 dieback crisis: genetic variation in resistance can prove a long-term solution. *Plant Pathology,*
722 *63,* 485-499. https://doi.org/10.1111/ppa.12196

723 Mitchell, C. E., Tilman, D. & Groth, J. V. (2002). Effects of grassland plant species diversity,
724 abundance, and composition on foliar fungal disease. *Ecology*, *83*, 1713-1726.
725 https://doi.org/10.1890/0012-9658(2002)083[1713:EOGPSD]2.0.CO;2

726 Mitchell, R. ., Bailey, S., Beaton, J. K., Bellamy, P. E., Brooker, R. W., Broome, A., Chetcuti, J., Eaton,
727 S., Ellis, C. J., Farren, J., Gimona, A., Goldberg, E., Hall, J., Harmer, R., Hester, A. J., Hewison, R.
728 L., Hodgetts, N. G., Hooper, R. J., Howe, L., … Woodward, S. (2014). The potential ecological
729 impact of ash dieback in the UK. *JNCC Report* No. 483.
730 https://hub.jncc.gov.uk/assets/1352bab5-3914-4a42-bb8a-a0a1e2b15f14

731 Muñoz, F., Marçais, B., Dufour, J., & Dowkiw, A. (2016). Rising out of the ashes: additive genetic
732 variation for crown and collar resistance to *Hymenoscyphus fraxineus* in *Fraxinus excelsior*.
733 *Phytopathology 106*, 1535–1543.

734 Murrell, D. J., & Law, R. (2003). Heteromyopia and the spatial coexistence of similar competitors.
735 *Ecology Letters, 6*, 48–59. https://doi.org/10.1046/j.1461-0248.2003.00397.x

736 Nemesio-Gorriz, M., McGuinness, B., Grant, J., Dowd, L., & Douglas, G. C. (2019). Lenticel infection in
737 *Fraxinus excelsior* shoots in the context of ash dieback. *IForest*, *12*, 160–165.
738 https://doi.org/10.3832/ifor2897-012

739 Pautasso, M., Holdenrieder, O., & Stenlid, J. (2005). Susceptibility to Fungal Pathogens of Forests
740 Differing in Tree Diversity. *Forest Diversity and Function*, *176*, 263–289.
741 https://doi.org/10.1007/3-540-26599-6_13

742 Pautasso, M., Aas, G., Queloz, V., & Holdenrieder, O. (2013). European ash (*Fraxinus excelsior*)
743 dieback - A conservation biology challenge. *Biological Conservation*, *158*, 37–49.
744 https://doi.org/10.1016/j.biocon.2012.08.026

745 Peterken, G., & Mountford, E. (2017). *Woodland development: A Long-term study of Lady Park*
746 *Wood*. CABI International, Wallingford.

747 Pommerening, A., & Grabarnik, P. (2019). *Individual-based Methods in Forest Ecology and*
748 *Management*. Springer, Dordrecht. https://doi.org/10.1007/978-3-030-24528-3

749 Pommerening, A., & Sánchez Meador, A. J. (2018). Tamm review : Tree interactions between myth
750 and reality. *Forest Ecology and Management*, *424*, 164–176.
751 https://doi.org/10.1016/j.foreco.2018.04.051

752 Pretzsch, H., Block, J., Dieler, J., Dong, P.H., Kohnle, U., Nagel, J., Spellman, H. & Zingg, A. (2010).
753 Comparison between the productivity of pure and mixed stands of Norway spruce and
754 European beech along an ecological gradient. *Ann. For. Sci., 67*, 712.

755 Queloz, V. (2016). Eschentriebsterben. Sterben ausgewachsene Eschen auch ab? *Wald und Holz,*
756 *97(6)*, 23-26.

757 R Core Team. (2021). R: A language and environment for statistical computing. R Foundation for
758 Statistical Computing.

759 Roberts, M., Gilligan, C. A., Kleczkowski, A., Hanley, N., Whalley, A. E., & Healey, J. R. (2020). The
760 Effect of Forest Management Options on Forest Resilience to Pathogens. *Frontiers in Forests*
761 *and Global Change*, *3,* 7. https://doi.org/10.3389/ffgc.2020.00007

762 Rutten, G., Hönig, L., Schwaß, R., Braun, U., Saadani, M., Schuldt, A., Michalski, S. G., & Bruelheide,
763 H. (2021). More diverse tree communities promote foliar fungal pathogen diversity, but
764 decrease infestation rates per tree species, in a subtropical biodiversity experiment. *Journal of*
765 *Ecology*, *109*, 2068–2080. https://doi.org/10.1111/1365-2745.13620

766 Schlegel, M., Queloz, V., & Sieber, T. N. (2018). The endophytic mycobiome of European ash and
767 sycamore maple leaves – geographic patterns, host specificity and influence of ash dieback.
768 *Frontiers in Microbiology*, *9*, 2345. https://doi.org/10.3389/fmicb.2018.02345

769 Sheil, D., Burslem, D. F. R. P., Alder, D. (1995). The interpretation and misinterpretation of mortality
770 rate measures. *Journal of Ecology*, *83*, 331-333. https://doi.org/10.2307/2261571

771 Skovsgaard, J.P., Thomsen, I.M., Skovsgaard, I.M., & Martinussen, T. (2010). Associations among
772 symptoms of dieback in even-aged stands of ash (*Fraxinus excelsior* L.). *Forest Pathology, 40*, 7–
773 18.

774 Skovsgaard, J. P., Wilhelm, G. J., Thomsen, I. M., Metzler, B., Kirisits, T., Havrdová, L., Enderle, R.,
775 Dobrowolska, D., Cleary, M., & Clark, J. (2017). Silvicultural strategies for *Fraxinus excelsior* in
776 response to dieback caused by *Hymenoscyphus fraxineus*. *Forestry*, *90*, 455–472.
777 https://doi.org/10.1093/forestry/cpx012

778 Stener, L.-G. (2018). Genetic evaluation of damage caused by ash dieback with emphasis on
779 selection stability over time. *Forest Ecology and Management*, *409*, 584–592.
780 https://doi.org/10.1016/j.foreco.2017.11.049

781 Stocks, J. J., Buggs, R. J. A, & Lee, S. J. (2017). A first assessment of *Fraxinus excelsior* (common ash)
782 susceptibility to *Hymenoscyphus fraxineus* (ash dieback) throughout the British Isles. *Scientific*
783 *Reports*, *7*, 16546. https://doi.org/10.1038/s41598-017-16706-6

784 Stocks, J. J., Metheringham, C. L., Plumb, W. J., Lee, S. J., Kelly, L. J., Nichols, R. A., & Buggs, R. J.
785 (2019). Genomic basis of European ash tree resistance to ash dieback fungus. *Nature Ecology &*
786 *Evolution*, *3*, 1686–1696. https://doi.org//10.1038/s41559-019-1036-6

787 Thomas, P. A. (2016). Biological Flora of the British Isles: *Fraxinus excelsior*. *Journal of Ecology*, *104*,
788 1158–1209. https://doi.org/10.1111/1365-2745.12566

789 Timmermann, V., Børja, I., Hietala, A. M., Kirisits, T., & Solheim, H. (2011). Ash dieback: Pathogen
790 spread and diurnal patterns of ascospore dispersal, with special emphasis on Norway. *EPPO*
791 *Bulletin*, *41*, 14–20. https://doi.org/10.1111/j.1365-2338.2010.02429.x

792 Timmermann, V., Nagy, N. E., Hietala, A. M., Børja, I., & Solheim, H. (2017). Progression of ash
793 dieback in Norway related to tree age, disease history and regional aspects. *Baltic Forestry*, *23*,
794 150–158.

795 Turczanski, K., Rutkowski, P., Dyderski, M. K., Wronska-Pilarek, D., & Nowinski, M. (2020). Soil pH
796 and organic matter content affects European ash (*Fraxinus excelsior* L.) crown defoliation and
797 its impact on understory vegetation. *Forests*, *11*, 22. https://doi.org/10.3390/F11010022

798 Wang, H., Zhang X., Hu, Y., & Pommerening, A. (2021). Spatial patterns of correlation between
799 conspecific species and size diversity in forest ecosystems. *Ecological Modelling*, 457, 109678.
800 https://doi.org/10.1016/j.ecolmodel.2021.109678

801 Wang, W., Chen, X., Zeng, W., Wang, J., & Meng, J. (2019). Development of a mixed-effects
802 individual-tree basal area increment model for oaks (*Quercus* spp.) considering forest structural
803 diversity. *Forests*, *10*, 474. https://doi.org/10.3390/f10060474

804 Wagenmakers, E. J. & Farrell, S. (2004). AIC model selection using Akaike weights. *Psychonomic*
805 *Bulletin & Review, 11*, 192-196.

806 Wykoff, W. (1990). A basal area increment model for individual conifers in the northern Rocky
807 Mountains. *Forest Science*, *26*, 1077–1104.

808 Zollner, A., & Kölling, C. (1994). Eschenkulturen auf ungeeigneten Standorten. *Allg. Forstz*, *2*, 61–64.

809 Zuur, A.F., Ieno, E.N., Walker, N., Saveliev, A.A., & Smith, G. (2009). *Mixed effects models and*
810 *extensions in ecology with R*. Springer, New York, NY. https://doi.org/10.1007/978-0-387-
811 87458-6

812
813
814

10. SUPPORTING INFORMATION

Additional supporting information may be found online in the Supporting Information section at https://doi.org/10.5061/dryad.ngf1vhhxg.